Thermal phonon scattering at singlet-triplet donor states in cubic semiconductors

A. Puhl, E. Sigmund, and J. Maier
Institut für Theoretische Physik, Universität Stuttgart,
Pfaffenwaldring 57, 7000 Stuttgart 80, Federal Republic of Germany
(Received 21 August 1984)

The mean phonon scattering rate at a localized electronic singlet-triplet system (e.g., the electronic ground state of group-V elements in germanium) is calculated using Green functions and transformation techniques. As a function of the singlet-triplet distance $4\Delta_0$, the resonant scattering process at the singlet-triplet transition is modulated by a dynamical scattering mechanism at the degenerated triplet state itself (Jahn-Teller effect). This modulation dominates for small $4\Delta_0$ and, leading to a strong temperature dependence of the scattering rate, reduces considerably the thermal conductivity. The results will be compared with thermal conductivity measurements of weakly n-doped semiconductors.

I. INTRODUCTION

The lattice thermal conductivity of semiconductors is strongly influenced by defects creating donor or acceptor states. For dilute impurity concentrations in many materials these electronic defect level structures cause additional scattering processes for low-frequency phonons in the meV range. The resulting decrease of the thermal conductivity at low temperatures has been detected for a large number of samples in recent years.[1,2] The intensities of the phonon scattering processes strongly depend upon both the electronic level structure of the defects as well as the character of the electron-phonon interaction between the defects and the phonon modes of the lattice.

In this paper we shall consider defects with a very specific electronic level structure, namely localized electronic singlet-triplet systems. Physical realizations of these structures are found in the valley-orbit-split ground states of the donors As, Sb, P, and Li in Ge. The structure is schematically drawn in Fig. 1.

On the energy scale the donor states are located just below the conduction band. The ground state, which is fourfold degenerate in cubic semiconductors, is split into a singlet and a triplet state, separated by the valley-orbit splitting $4\Delta_0$. Characteristic values of the valley-orbit splitting for some donors in Ge are listed in Table I.

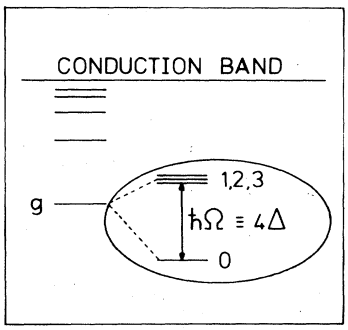

FIG. 1. Energy levels of group-V elements such as Sb, P, or As in a germanium lattice (schematically drawn). The ground state g is split into a singlet and a triplet state ("valley-orbit splitting" $4\Delta_0$).

For a detailed discussion of the standard theory of shallow impurity states in semiconductors, the effective mass theory, we refer to the article of Kohn.[4] A special feature of these defects is the large extension of the defect wave function ψ, characterized by the Bohr radius a^* (~ 40 Å). ψ is approximated by a hydrogentype function.

In the following we shall discuss the scattering of phonons in these systems which can theoretically be described by a relaxation rate τ^{-1}, which has so far been calculated on the basis of peturbation theory by Keyes,[5] Griffin and Carruthers,[3] and Suzuki and Mikoshiba.[6] Indeed perturbation theory in second-order Born approximation considers mainly the resonant transition scattering process between the singlet and triplet states, but neglects, however, the dynamical Jahn-Teller effect (JTE) at the degenerate triplet state itself.[7] As shown in a previous paper by two of the authors[8] the JTE leads to an additional dynamical scattering process with a strong temperature dependence and therefore with a strong influence on the thermal conductivity. In a simplified manner this dynamical scattering mechanism can be explained in the following way.

The triply degenerate electronic level can couple to doubly (e) and triply (t) degenerate lattice vibrations (JTE). Via the electron-phonon interaction the lattice vibrations cause a time-dependent oscillating splitting $\Delta(t)$ of the electronic triplet state into a singlet and a doublet state. Averaging over a long time period the splitting $\Delta(t)$ is zero [$\langle \Delta(t) \rangle_{av}=0$]. When an incident phonon reaches the defect ion, however, a momentary electronic level splitting occurs and therefore the phonon can be scattered. From this simple model we can draw two conclusions.

(1) Because all coupled phonon modes of the crystal are involved in this dynamic level motion the results (scattering rate, etc.) are strongly temperature dependent.

(2) This dynamical process cannot be described in second-order perturbation theory.

TABLE I. Values for the spin-orbit splitting used in our calculations (Refs. 2 and 3).

	Sb	P	As	Li
$4\Delta_0=\hbar\Omega$ (meV)	0.32	2.83	4.23	−0.12
Ω (THz)	0.49	4.30	6.43	−0.18

In this paper we are mainly interested in the influence of resonant scattering at the singlet-triplet system on the dynamical scattering due to the JTE of the triplet state. Especially when the triplet state is occupied with high probability, i.e., $4\Delta_0$ is small or even negative, we shall expect an important contribution from the JTE to the total phonon scattering process.

In order to include the dynamical JTE we intend to calculate the phonon relaxation rate τ^{-1} with the help of higher-order Green functions, a technique which has already been successfully applied to Γ_8 acceptor states.[7–9] We finally calculate the thermal conductivity of specific systems like Ge(Sb) and Ge(As) without using fitting parameters, and we compare our results with experimental data.

II. MODEL HAMILTONIAN

The total Hamiltonian H describing a defect atom in an octahedral crystal contains three parts:

$$H = H_{\text{el}} + H_{\text{ph}} + H_{\text{el-ph}} \,. \tag{2.1}$$

Since we take as a basis an electronic singlet-triplet system for the impurity atom (see Fig. 1) we write for the electronic Hamiltonian ($\hbar\Omega = 4\Delta_0$)

$$H_{\text{el}} = \frac{\hbar\Omega}{4}\sigma_{15} \,. \tag{2.2}$$

σ_{15} is one of the quasispin operators building up the SU(4) algebra. Their connection with the four electronic state operators is given in Tables II and III.

The unperturbed phonon Hamiltonian reads

$$H_{\text{ph}} = \sum_p \hbar\omega_p b_p^\dagger b_p \,, \tag{2.3}$$

where we sum over all phonon modes $p \equiv q\lambda$ (q is the phonon wave vector, λ is acoustic branch l, t_1, or t_2). b_p and $b_p^\dagger$ are Bose creation and annihilation operators and commute in the following way:

TABLE II. The commutators $[\sigma_i, \sigma_j]$ of the 15 SU(4) operators for $j = 1, \ldots, 8$ and (a) $i, \ldots, 8$, (b) $i = 9, \ldots, 15$. The result has to be multiplied by the imaginary number i.

(a)

σ_i \ σ_j	σ_1	σ_2	σ_3	σ_4	σ_5	σ_6	σ_7	σ_8
σ_1	0	$-\sigma_{11}$	σ_{10}	$\sqrt{3}\sigma_9$	σ_9	0	$-\sigma_{12}$	$-\sigma_{13}$
σ_2	σ_{11}	0	$-\sigma_9$	$-\sqrt{3}\sigma_{10}$	$-\sigma_{10}$	$-\sigma_{12}$	0	$-\sigma_{14}$
σ_3	$-\sigma_{10}$	σ_9	0	0	$-2\sigma_{11}$	$-\sigma_{13}$	$-\sigma_{14}$	0
σ_4	$-\sqrt{3}\sigma_9$	$\sqrt{3}\sigma_{10}$	0	0	0	$\frac{1}{\sqrt{3}}\sigma_{14}$	$\frac{1}{\sqrt{3}}\sigma_{13}$	$-\frac{2}{\sqrt{3}}\sigma_{12}$
σ_5	$-\sigma_9$	$-\sigma_{10}$	$2\sigma_{11}$	0	0	$-\sigma_{14}$	σ_{13}	0
σ_6	0	σ_{12}	σ_{13}	$-\frac{1}{\sqrt{3}}\sigma_{14}$	σ_{14}	0	σ_{11}	$-\sigma_{10}$
σ_7	σ_{12}	0	σ_{14}	$-\frac{1}{\sqrt{3}}\sigma_{13}$	$-\sigma_{13}$	$-\sigma_{11}$	0	σ_9
σ_8	σ_{13}	σ_{14}	0	$\frac{2}{\sqrt{3}}\sigma_{12}$	0	σ_{10}	$-\sigma_9$	0

(b)

σ_i \ σ_j	σ_1	σ_2	σ_3	σ_4	σ_5	σ_6	σ_7	σ_8
σ_9	$\sigma_5 + \sqrt{3}\sigma_4$	$-\sigma_3$	σ_2	$-\sqrt{3}\sigma_1$	$-\sigma_1$	0	σ_8	$-\sigma_7$
σ_{10}	σ_3	$\sigma_5 - \sqrt{3}\sigma_4$	$-\sigma_1$	$\sqrt{3}\sigma_2$	$-\sigma_2$	$-\sigma_8$	0	σ_6
σ_{11}	$-\sigma_2$	σ_1	$-2\sigma_5$	0	$2\sigma_3$	σ_7	$-\sigma_6$	0
σ_{12}	$-\sigma_7$	$-\sigma_6$	0	$-\frac{2}{\sqrt{3}}\sigma_8$	0	σ_2	$\sigma_1 + \frac{2}{3}\sigma_{15}$	$\frac{2}{\sqrt{3}}\sigma_4$
σ_{13}	$-\sigma_8$	0	$-\sigma_6$	$\frac{1}{\sqrt{3}}\sigma_7$	σ_7	$\sigma_3 + \frac{2}{3}\sigma_{15}$	$-\frac{1}{\sqrt{3}}\sigma_4 - \sigma_3$	σ_1
σ_{14}	0	$-\sigma_8$	$-\sigma_7$	$\frac{1}{\sqrt{3}}\sigma_6$	$-\sigma_6$	$-\frac{1}{\sqrt{3}}\sigma_4 + \sigma_5$	σ_3	σ_2
σ_{15}	0	0	0	0	0	$-4\sigma_{14}$	$-4\sigma_{13}$	$-4\sigma_{12}$

TABLE III. Anticommutation relations $[\sigma_i,\sigma_j]_+$ of the 15 SU(4) operators for $j=1,\ldots,8$ and (a) $i=1,\ldots,8$, (b) $i=9,\ldots,15$.

(a)

σ_i \ σ_j	σ_1	σ_2	σ_3	σ_4	σ_5	σ_6	σ_7	σ_8
σ_1	$2a_2^\dagger a_2+2a_3^\dagger a_3$	σ_3	σ_2	$\frac{1}{\sqrt{3}}\sigma_1$	$-\sigma_1$	0	σ_8	σ_7
σ_2	σ_3	$2a_1^\dagger a_1+2a_3^\dagger a_3$	σ_1	$\frac{1}{\sqrt{3}}\sigma_2$	σ_2	σ_8	0	σ_6
σ_3	σ_2	σ_1	$2a_1^\dagger a_1+2a_2^\dagger a_2$	$-\frac{2}{\sqrt{3}}\sigma_3$	0	σ_7	σ_6	0
σ_4	$\frac{1}{\sqrt{3}}\sigma_1$	$\frac{1}{\sqrt{3}}\sigma_2$	$-\frac{2}{\sqrt{3}}\sigma_3$	$\frac{2}{3}a_1^\dagger a_1+\frac{2}{3}a_2^\dagger a_2+\frac{2}{3}a_3^\dagger a_3$	$-\frac{2}{\sqrt{3}}\sigma_5$	$-\frac{1}{\sqrt{3}}\sigma_6$	$-\frac{1}{\sqrt{3}}\sigma_7$	$\frac{2}{\sqrt{3}}\sigma_8$
σ_5	$-\sigma_1$	σ_2	0	$-\frac{2}{\sqrt{3}}\sigma_5$	$2a_1^\dagger a_1+2a_2^\dagger a_2$	σ_6	$-\sigma_7$	0
σ_6	0	σ_8	σ_7	$-\frac{1}{\sqrt{3}}\sigma_6$	σ_6	$2a_0a_0+2a_1^\dagger a_1$	σ_3	σ_2
σ_7	σ_8	0	σ_6	$-\frac{1}{\sqrt{3}}\sigma_7$	σ_7	σ_3	$2a_0^\dagger a_0+2a_2^\dagger a_2$	σ_1
σ_8	σ_7	σ_6	0	$\frac{2}{\sqrt{3}}\sigma_8$	0	σ_2	σ_1	$2a_0^\dagger a_0+2a_3^\dagger a_3$

(b)

σ_i \ σ_j	σ_1	σ_2	σ_3	σ_4	σ_5	σ_6	σ_7	σ_8
σ_9	0	$-\sigma_{11}$	$-\sigma_{10}$	$\frac{1}{\sqrt{3}}\sigma_9$	$-\sigma_9$	0	σ_{12}	$-\sigma_{13}$
σ_{10}	$-\sigma_{11}$	0	$-\sigma_9$	$\frac{1}{\sqrt{3}}\sigma_{10}$	σ_{10}	$-\sigma_{12}$	0	σ_{14}
σ_{11}	$-\sigma_{10}$	$-\sigma_9$	0	$-\frac{2}{\sqrt{3}}\sigma_{11}$	0	σ_{13}	$-\sigma_{14}$	0
σ_{12}	σ_{13}	σ_{14}	0	$\frac{2}{\sqrt{3}}\sigma_{12}$	0	$-\sigma_{10}$	σ_9	0
σ_{13}	σ_{12}	0	σ_{14}	$-\frac{1}{\sqrt{3}}\sigma_{13}$	$-\sigma_{13}$	σ_{11}	0	σ_9
σ_{14}	0	σ_{12}	σ_{13}	$-\frac{1}{\sqrt{3}}\sigma_{14}$	σ_{14}	0	$-\sigma_{11}$	σ_{10}
σ_{15}	$2\sigma_1$	$2\sigma_2$	$2\sigma_3$	$2\sigma_4$	$2\sigma_5$	$-2\sigma_6$	$-2\sigma_7$	$-2\sigma_8$

$$[b_p,b_{p'}^\dagger]=\delta_{pp'}\,,$$
$$[b_p,b_{p'}]=[b_p^\dagger,b_{p'}^\dagger]=0\,. \tag{2.4}$$

The electron-phonon interaction between the defect atom and the crystal lattice can be derived by group-theoretical arguments:

$$H_{\text{el-ph}}=\hbar\sum_p \Lambda^p(b_p^\dagger+b_p)\,,$$

where we make use of the abbreviations

$$\Lambda^p=\sum_{i=1}^{8}\phi_i^p\sigma_i\,, \tag{2.5}$$
$$\phi_i^p=f(q)D_tS_i^p \quad \text{for } i=1,2,3$$
$$\phi_i^p=f(q)D_eS_i^p \quad \text{for } i=4,5 \tag{2.6}$$
$$\phi_i^p=f(q)B_tS_{i-5}^p \quad \text{for } i=6,7,8\,.$$

The $\sigma_1,\ldots,\sigma_{15}$ are quasispin operators representing a SU(4) Lie algebra. Their commutation and anticommutation relations are listed in Tables II and III.

Furthermore the S_i^p $(i=1,2,3)$ and S_i^p $(i=4,5)$ project the lattice phonons onto the symmetry coordinates of t_{2g} and e_g vibrations, respectively:[10]

$$S_1^p=\left[\frac{\hbar\omega_p}{2Mc_\lambda^2}\right]^{1/2}\frac{1}{\sqrt{3}}(q_z e_{\lambda y}+q_y e_{\lambda z}) ,$$
$$S_2^p=\left[\frac{\hbar\omega_p}{2Mc_\lambda^2}\right]^{1/2}\frac{1}{\sqrt{3}}(q_z e_{\lambda x}+q_x e_{\lambda z}) ,$$
$$S_3^p=\left[\frac{\hbar\omega_p}{2Mc_\lambda^2}\right]^{1/2}\frac{1}{\sqrt{3}}(q_x e_{\lambda y}+q_y e_{\lambda x}) , \quad (2.7)$$
$$S_4^p=\left[\frac{\hbar\omega_p}{2Mc_\lambda^2}\right]^{1/2}\frac{1}{\sqrt{3}}(2q_z e_{\lambda z}-q_x e_{\lambda x}-q_y e_{\lambda y}) ,$$
$$S_5^p=\left[\frac{\hbar\omega_p}{2Mc_\lambda^2}\right]^{1/2}\frac{1}{\sqrt{3}}(q_x e_{\lambda x}-q_y e_{\lambda y}) .$$

Here ω_p denotes the frequency and c_λ the velocity of the corresponding phonon. M is the mass of the crystal. (q_x,q_y,q_z) signifies the unit vector along q and $(e_{\lambda x},e_{\lambda y},e_{\lambda z})$ the polarization vector for the phonon branch λ.

In (2.6) we discern three coupling terms which are ruled by the deformation potential constants D_e, D_t, and B_t: the D_e and D_t terms describe the coupling of longitudinal e_g phonons and transverse t_{2g} phonons, respectively, at the degenerate triplet level itself, whereas the B_t term corresponds to the coupling of transverse t_{2g} phonons at the singlet-triplet transition.

Comparison with static stress experiments[11] leads to the following result concerning the deformation potentials of donors in germanium:[12]

$$B_t=D_t . \quad (2.8)$$

As a matter of fact, D_e is much smaller than D_t or B_t. Therefore the coupling of longitudinal e_g phonons at the triplet state is very weak and can be neglected.[13]

Finally, the coupling function $f(q)$ in (2.6) leads to a cutoff for high-frequency phonons. The simplest treatment of $f(q)$ is within the effective mass approximation,[4,14] where the donor wave functions are determined by a hydrogenlike model. Considering only the s-type parts of the electronic ground state one arrives at

$$f(q)=[1+\tfrac{1}{4}(a^*q)^2]^{-2} , \quad (2.9)$$

where a^* is the Bohr radius of the defect, i.e., a measure of the extent of the donor wave function.[15]

III. THE PHONON SCATTERING RATE

In addition to the usual phonon scattering processes in crystals[16]—e.g., phonon-phonon interaction, boundary scattering, and isotopic scattering— donors in semiconductors give rise to scattering due to the electron-phonon interaction.

The scattering rate (or inverse lifetime) τ^{-1} for a single phonon mode $p\equiv q\lambda$ is related to the imaginary part of the T matrix[17,18] as follows:

$$\tau_p^{-1}=-\omega_p^{-1}\lim_{\epsilon\to 0}\mathrm{Im}[T_{pp}(\omega_p+i\epsilon)] . \quad (3.1)$$

The T matrix itself is defined by the relation

$$G=G_0-G_0TG_0 , \quad (3.2)$$

where G_0 and G are the phonon Green functions of the unperturbed and perturbed crystal, respectively.

Using the technique of double-time thermodynamic Green functions by Zubarev[19,20] we can write G as a dynamical susceptibility:

$$G_{pp'}(\omega)=\pi(\omega_p\omega_{p'})^{-1/2}\langle\langle Q_p;Q_{p'}\rangle\rangle . \quad (3.3)$$

With this formalism we finally express the scattering rate by Green functions of the quasispin operators $\sigma_1,\ldots,\sigma_8$ as[7,8,18]

$$\tau_p^{-1}=4\pi\frac{nV}{Z_A}\mathrm{Im}\langle\langle\Lambda^p;\Lambda^p\rangle\rangle . \quad (3.4)$$

Z_A is the number of atoms in the crystal, n the defect concentration, and V the crystal volume.

In a good approximation we can confine ourselves to the calculation of τ_p^{-1} for phonons in the z direction, assuming that every other direction gives approximately the same scattering rate. In this way we can avoid the task of averaging over all q. Thus we arrive at

$$\tau_l^{-1}=\frac{8\pi}{g}\frac{n}{Z_A\rho_M}\frac{\hbar\omega}{c_l^2}D_e^2 f_l(\omega)\mathrm{Im}G_l(\omega) , \quad (3.5)$$

$$\tau_t^{-1}=\frac{2\pi}{3}\frac{n}{Z_A\rho_M}\frac{\hbar\omega}{c_t^2}D_t^2 f_t(\omega)\mathrm{Im}G_t(\omega) , \quad (3.6)$$

where we have used the Debye approximation $\omega=cq$, ρ_M denotes the crystal mass density, and G_l and G_t are abbreviations for the spin Green functions

$$G_l=\langle\langle\sigma_4;\sigma_4\rangle\rangle , \quad (3.7)$$

$$G_t=\langle\langle\sigma_2;\sigma_2\rangle\rangle+\langle\langle\sigma_7;\sigma_7\rangle\rangle+\langle\langle\sigma_2;\sigma_7\rangle\rangle+\langle\langle\sigma_7;\sigma_2\rangle\rangle . \quad (3.8)$$

IV. THERMAL AVERAGES

We shall calculate thermal averages $\langle A\rangle=\mathrm{tr}(A\rho)$ in a transformed space, using an exponential transformation $U=e^S$ of the form[21,22]

$$S=\sum_p\omega_p^{-1}\left[\sum_{i=1}^{5}\phi_i^p\sigma_i\right]P_p+\sum_p\frac{\omega_p}{\omega_p^2-\Omega^2}\left[\sum_{i=1}^{8}\phi_i^p\sigma_i\right]P_p$$
$$-i\sum_p\Omega_{\omega_p^2-\Omega^2}(\phi_6^p\sigma_{14}+\phi_7^p\sigma_{13}+\phi_8^p\sigma_{12}) \quad (4.1)$$

which guarantees that the transformed Hamiltonian $\tilde{H}=e^{-S}He^S$ no longer contains linear terms in the coupling constants.

Taking as a basis Boltzmann-distributed occupation numbers for the singlet (n_0) and the triple (n_1) as follows,

$$n_0=[1+3\exp(\hbar\Omega/k_BT)]^{-1} ,$$
$$n_1=\tfrac{1}{3}(1-n_0) , \quad (4.2)$$

we can develop the thermal averages up to linear terms in the coupling constants using Bose statistics for the phonons:

$$\langle P_p Q_{p'} \rangle = \delta_{pp'} , \tag{4.3a}$$

$$\langle Q_p Q_{p'} \rangle = \delta_{pp'} L_p , \quad L_p = \coth \frac{\hbar \omega_p}{2 k_B T} \tag{4.3b}$$

$$\langle P_p P_{p'} \rangle = - \langle Q_p Q_{p'} \rangle , \tag{4.3c}$$

$$\langle Q_p \sigma_i \rangle = \begin{cases} -\dfrac{4\pi}{\omega_p} \phi_i^p & \text{for } i = 1, \ldots, 5 \\ -\dfrac{2(n_0+n_1)}{\omega_p^2 - \Omega^2} \omega_p Q_i^p & \text{for } i = 6,7,8 \\ 0 & \text{for } i = 9, \ldots, 15 \end{cases} \tag{4.3d}$$

$$\langle P_p \sigma_i \rangle = -i \frac{2\Omega(m_0+n_1)}{\omega_p^2 - \Omega^2} \times \begin{cases} \phi_6^p & \text{for } i = 14 \\ \phi_7^p & \text{for } i = 13 \\ \phi_8^p & \text{for } i = 12 \end{cases} \tag{4.3e}$$

$$\langle \sigma_i \rangle = \begin{cases} -3(n_0 - n_1) & \text{for } i = 15 \\ 0 & \text{for } i = 1, \ldots, 14 \end{cases} \tag{4.3f}$$

$$\langle \sigma_i \sigma_j \rangle = \delta_{ij} \times \begin{cases} 2n_1 & \text{for } i = 1, \ldots, 5 \text{ and } 9, \ldots, 11 \\ n_0 + n_1 & \text{for } i = 6,7,8,12,13 \\ 3(3n_0 + n_1) & \text{for } i = 15 . \end{cases} \tag{4.3g}$$

V. EVALUATION OF SPIN GREEN FUNCTIONS

In the following we calculate the inverse lifetime of transverse phonons as given by (3.6) and we are left with the evaluation of the four spin Green functions denoted by G_t in (3.8). The formal procedure of the calculation will be illustrated for the Green function $\langle\langle \sigma_2;\sigma_j \rangle\rangle$ (with $j=2,7$) using the equation-of-motion method as follows.[19,20]

The first hierarchy reads

$$\omega \langle\langle \sigma_2;\sigma_j \rangle\rangle = \sum_p \langle\langle Q_p[\sigma_2,\Lambda^p];\sigma_j \rangle\rangle \tag{5.1}$$

and further development leads to

$$\begin{aligned} (\omega^2 - \omega_p^2) \langle\langle Q_p[\sigma_2,\Lambda^p];\sigma_j \rangle\rangle = {} & \frac{\omega}{2\pi} \langle Q_p[[\sigma_2,\Lambda^p],\sigma_j] \rangle + \omega \sum_{p'} \langle\langle Q_p Q_{p'}[[\sigma_2,\Lambda^p],\Lambda^{p'}];\sigma_j \rangle\rangle \\ & + \omega_p \sum_{p'} \langle\langle P_p Q_{p'}[[\sigma_2,\Lambda^p],\Lambda^{p'}];\sigma_j \rangle\rangle + 2\omega_p \langle\langle \Lambda^p[\sigma_2,\Lambda^p];\sigma_j \rangle\rangle \\ & + \hbar^{-1} \langle\langle (\omega Q_p + \omega_p P_p)[[\sigma_2,\Lambda^p];H_{\mathrm{el}}];\sigma_j \rangle\rangle . \end{aligned} \tag{5.2}$$

We now make use of the identity

$$2AB = [A,B] + [A,B]_+ \tag{5.3}$$

and the random-phase approximation (RPA)

$$\langle\langle Q,Q',\ldots;\sigma_j \rangle\rangle = L_p \delta_{pp'} \langle\langle \ldots;\sigma_j \rangle\rangle , \tag{5.4}$$

$$\langle\langle P,Q',\ldots;\sigma_j \rangle\rangle = \delta_{pp'} \langle\langle \ldots;\sigma_j \rangle\rangle , \tag{5.5}$$

to combine (5.1) and (5.2) yielding

$$\begin{aligned} \langle\langle \sigma_2;\sigma_j \rangle\rangle = {} & \sum_p \frac{\langle Q_p[[\sigma_2,\Lambda^p],\sigma_j] \rangle}{2\pi(\omega^2 - \omega_p^2)} + \sum_p \frac{L_p}{\omega^2 - \omega_p^2} \langle\langle [[\sigma_2,\Lambda^p],\Lambda^p];\sigma_j \rangle\rangle \\ & + \sum_p \frac{\omega_p}{\omega(\omega^2 - \omega_p^2)} \langle\langle [[\sigma_2,\Lambda^p],\Lambda^p]_+;\sigma_j \rangle\rangle - \sum_p \frac{\Omega}{\omega^2 - \omega_p^2} \left\langle\!\!\left\langle \left[Q_p + \frac{\omega}{\omega_p} P_p \right] (\phi_6^p \sigma_8 + \phi_8^p \sigma_6);\sigma_j \right\rangle\!\!\right\rangle . \end{aligned} \tag{5.6}$$

The calculation of $[[\sigma_2,\Lambda],\Lambda]_\pm$ will be carried out with the condition that orthogonal terms like $(\phi_1^p \phi_2^p)$ do not contribute when summing over p. We can therefore write for $\langle\langle \sigma_2;\sigma_j \rangle\rangle$ (see Appendix A)

$$(1-A) \langle\langle \sigma_2;\sigma_j \rangle\rangle - b_2^j - A \langle\langle \sigma_7;\sigma_j \rangle\rangle - \sum_p \frac{\Omega}{\omega^2 - \omega_p^2} \left\langle\!\!\left\langle \left[Q + \frac{\omega_p}{\omega} P \right] (\phi_6^p \sigma_8 + \phi_8^p \sigma_6);\sigma_j \right\rangle\!\!\right\rangle . \tag{5.7}$$

The third term in Eq. (5.7) contains Green functions of the type $\langle\langle Q_p \sigma_i;\sigma_j \rangle\rangle$ or $\langle\langle P_p \sigma_i;\sigma_j \rangle\rangle$ ($i=6,7,8$; $j=2,7$). A direct evaluation of these terms leads to a very complicated structure of the hierarchy. In addition a consistent treatment of these Green functions should include use of the RPA in higher hierarchies. Thus $\langle\langle Q_p \sigma_i;\sigma_j \rangle\rangle$ and $\langle\langle P_p \sigma_i;\sigma_j \rangle\rangle$ will be omitted in future.

In a similar way we proceed with the remaining three Green functions in Eq. (3.10) which can be expressed as a linear combination of $\langle\langle \sigma_2;\sigma_j \rangle\rangle$, $\langle\langle \sigma_{10};\sigma_j \rangle\rangle$, $\langle\langle \sigma_7;\sigma_j \rangle\rangle$, and $\langle\langle \sigma_{13};\sigma_j \rangle\rangle$. We finally obtain a system of linear equations (see Appendix A)

$$\begin{pmatrix} -b_1^j \\ -b_2^j \\ -b_3^j \\ -b_4^j \end{pmatrix} = \begin{pmatrix} -a_1 & 0 & -A & 0 \\ 0 & -a_2 & 0 & B \\ -A & \frac{i\Omega}{\omega}B & -a_3 & \frac{i\Omega}{\omega}D \\ \frac{i\Omega}{\omega}A & B & -\frac{i\Omega}{\omega}A & -a_4 \end{pmatrix} \begin{pmatrix} \langle\langle \sigma_2;\sigma_j \rangle\rangle \\ \langle\langle \sigma_{10};\sigma_j \rangle\rangle \\ \langle\langle \sigma_7;\sigma_j \rangle\rangle \\ \langle\langle \sigma_{13};\sigma_j \rangle\rangle \end{pmatrix} . \tag{5.8}$$

It must be pointed out that we are dealing with a problem involving two different types of scattering processes. One is related to the dynamical Jahn-Teller scattering at the degenerate triplet state [case (a)] and the other to the resonant scattering at the singlet-triplet transition [case (b)]. These two processes, however, cannot be separated physically nor in a mathematically exact way. Nevertheless, case (a) could be approximated by the Green function $\langle\langle \sigma_2;\sigma_2 \rangle\rangle$ and case (b) by $\langle\langle \sigma_7;\sigma_7 \rangle\rangle$. Let us mention that case (b) can be calculated in SU(2) algebra for a pure two-level system[17] and case (a) in SU(3) algebra for a pure triplet system.

We therefore solve (5.8) approximately up to second order in the deformation potentials and find

$$\langle\langle \sigma_2;\sigma_2 \rangle\rangle = \frac{b_1^2}{1-A-D} ,$$
$$\langle\langle \sigma_7;\sigma_7 \rangle\rangle = \frac{b_3^7}{1-\frac{\Omega^2}{\omega^2}-A-D} . \tag{5.9}$$

These Green functions fulfill the symmetry condition

$$\langle\langle B;A \rangle\rangle(\omega) = \langle\langle A;B \rangle\rangle(-\omega) . \tag{5.10}$$

The Green functions $\langle\langle \sigma_2;\sigma_7 \rangle\rangle$ and $\langle\langle \sigma_7;\sigma_2 \rangle\rangle$ are neglected in our treatment, because they contribute to higher orders of the Green function hierarchy only, if one demands the same accuracy as that for (5.9).

For the final evaluation we convert sums into integrals (continuum approximation) and seek the solution (see Appendix B):

$$\mathrm{Im}\langle\langle \sigma_2;\sigma_2 \rangle\rangle = \frac{[\omega^2-\Delta(\omega)]\beta(\omega)-\alpha(\omega)\Gamma(\omega)}{[\omega^2-\Delta(\omega)]^2+\Gamma(\omega)^2} , \tag{5.11}$$

$$\mathrm{Im}\langle\langle \sigma_7;\sigma_7 \rangle\rangle = \frac{\alpha'(\omega)\Gamma'(\omega)}{[\omega^2-\Omega^2-\Delta'(\omega)]^2+\Gamma'(\omega)^2} , \tag{5.12}$$

where we have neglected multiple-singularity terms which turned out to be of minor importance. Figures 2 and 3 graphically demonstrate the phonon scattering rate $\tau^{-1}(\omega)$ following from (3.6), (3.8), and (5.12). Figure 2 shows $\tau^{-1}(\omega)$ for different positive singlet-triplet distances $\Omega \equiv 4\Delta_0/\hbar$. The large width of the resonances is due to the dynamical JTE. Figure 3 proves well the influence of the dynamical JTE as a function of the triplet occupation probability, which is much higher for negative singlet-triplet distance. In case (a) the triplet state lies above the singlet state ($\Omega = +7$ THz$\hat{=}$4.6 meV) whereas in case (b) the structure is inverted ($\Omega = -7$ MHz), i.e., the singlet lies above the triplet. The resonant scattering process at the singlet-triplet transition, however, is not affected.

VI. THERMAL CONDUCTIVITY

Finally, we shall calculate the thermal conductivity for the samples Ge(As) and Ge(Sb) according to the semiphenomenological theories of Klemens[23] and Callaway[16] as

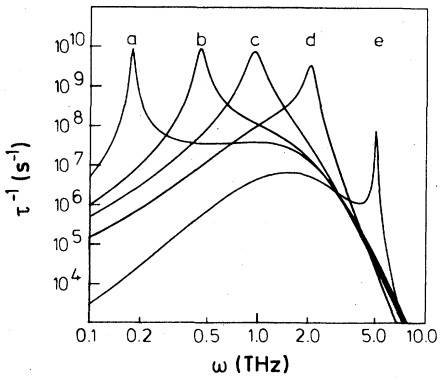

FIG. 2. Phonon scattering rate τ^{-1} as a function of phonon frequency ω with the following parameters: $a^* = 30$ Å, $T = 5$ K, $\hbar D_t = 5.5$ eV, $n = 10^{16}$ cm^{-3}. Curves a, b, c, d, and e belong to the singlet-triplet distances $\Omega = 0.2$, 0.5, 1.0, 2.0, and 5.0 THz) or $\hbar\Omega = 0.13$, 0.33, 0.66, 1.32, and 3.29 MeV, respectively.

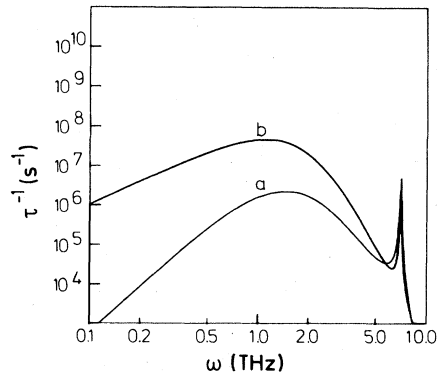

FIG. 3. Phonon scattering rate τ^{-1} as a function of phonon frequency ω with the same parameters as in Fig. 2. Curve a corresponds to $\Omega = 7$ THz ($\hat{=}$4.6 meV) and curve b to $\Omega = -7$ THz. In the latter case the triplet state, lying below the singlet state, is occupied with higher probability and leads to a stronger dynamical scattering process.

$$K(T)=\frac{k_B^4 T^3}{6\pi^2\hbar^3}\sum_\lambda c_\lambda^{-1}\int_0^\infty \frac{x^4 e^x}{(e^x-1)^2}\frac{1}{\tau_{\text{tot},\lambda}^{-1}}dx \ . \quad (6.1)$$

$\tau_{\text{tot},\lambda}^{-1}$ is the total inverse lifetime of all different and independent phonon scattering processes expressed by

$$\tau_{\text{tot},\lambda}^{-1}=\tau_I^{-1}+\tau_{B,\lambda}^{-1}+\tau_u^{-1}+\tau_{\text{el-ph},\lambda}^{-1} \ ,$$

where τ_I^{-1}, $\tau_{B,\lambda}^{-1}$, and τ_n^{-1} are the relaxation rates for isotropic, boundary, and umklapp scattering, respectively.[8,23] For simplicity in the numerical treatment for $\tau_{\text{el-ph},t}^{-1}$ as well as for $\tau_{\text{el-ph},l}^{-1}$ we used the result derived from Eq. (3.6). In our theory we did not make use of any fit parameter. On the contrary every physical parameter has been separately measured and can be found, e.g., in the paper of Bird and Pearlman.[1] These authors have measured the thermal conductivity of highly Sb-, P-, and As-doped germanium in a temperature range between 0.3 and 4.2 K. Their results (dashed lines) in comparison with our theoretical calculations (solid lines) are shown in Figs. 4 and 5. For As-doped germanium (Fig. 4) the singlet-triplet distance ($\hbar\Omega\equiv 4\Delta_0=4.23$ meV) is rather large. Thus as a consequence of the low triplet occupation probability the dynamical scattering process (JTE) scarcely contributes. Indeed the resonant scattering process between the singlet-triplet transition dominates here and we could handle Ge(As) as a two-level system.

Figure 4 includes also the curve c for a hypothetical system with an inverted singlet-triplet structure ($\Omega<0$) to demonstrate the influence of the dynamical JTE in the case of a high triplet occupation probability. Considering

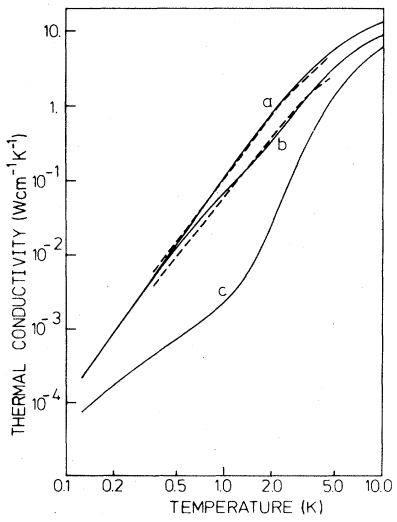

FIG. 4. Experimental (Ref. 1, dashed curves) and calculated (solid lines) thermal conductivity curves for As-doped germanium with the following physical parameters: curve a, $n=0$ (no doping); curve b, $n=2.7\times10^{16}$ cm^{-3}, $a^*=37$ Å, $\hbar D_t=5.5$ eV, $\hbar\Omega=4.23$ meV; curve c, same as curve b but $\hbar\Omega=-4.23$ MeV (inverted singlet-triplet structure).

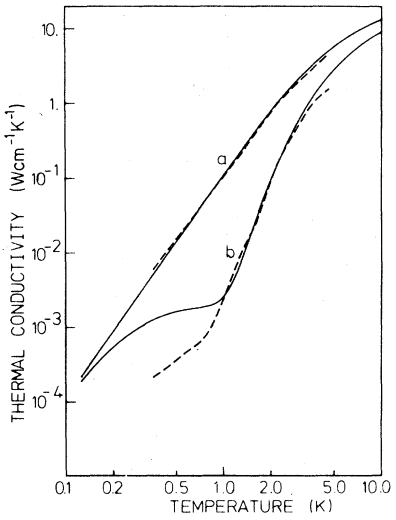

FIG. 5. Experimental (Ref. 1, dashed curves) and calculated (solid lines) thermal conductivity curves for Sb-doped germanium with the following parameters: curve a, $n=0$ (no doping); curve b, $n=3.0\times10^{16}$ cm^{-3}, $a^*=44$ Å, $\hbar D_t=4.4$ eV, $\hbar\Omega=0.32$ meV.

Sb-doped germanium (Fig. 5), where the singlet-triplet distance ($\hbar\Omega=0.32$ meV) is about 13 times smaller than for Ge(As), the dynamical scattering process at the higher occupied triplet state plays now a dominant role. As a consequence we observe a strongly reduced thermal conductivity.

Although the low-temperature thermal conductivity can be well explained by the method of Green functions, the mechanism for scattering of low-frequency phonons effective below 1 K has still not been found. This may be due to phonon scattering at a statically split triplet state due to internal strains. In the theoretical curves shown here this extra scattering effect is not included.

VII. CONCLUSIONS

The phonon scattering rate τ^{-1} has so far been calculated on the basis of perturbation theory.[3,5,6] Indeed perturbation theory in second-order Born approximation considers mainly the resonant transition scattering process between the singlet and triplet states, but neglects the dynamical Jahn-Teller effect at the degenerate triplet state itself. We performed a high-order Green-function calculation in order to include the additional dynamical scattering process due to the Jahn-Teller effect. This process is strongly temperature dependent and therefore has a great influence on the thermal conductivity. This influence is greater for smaller values of $4\Delta_0$ or for negative values, i.e., when the triplet state lies below the singlet state.

ACKNOWLEDGMENTS

The authors want to thank the Deutsche Forschungsgemeinschaft (DFG) for financial support. They would also like to thank C. Durst for a critical reading of the manuscript.

APPENDIX A

The definitions of terms used in deriving the system of linear equations, Eq. (5.8), are as follows:

$$L_p=\coth\frac{\hbar\omega_p}{2k_BT}\ ,$$

$$A=\sum_p\frac{L_p}{\omega^2-\omega_p^2}(\phi_1^p\phi_1^p+\phi_3^p\phi_3^p+\phi_6^p\phi_6^p+\phi_8^p\phi_8^p)\ ,$$

$$B=\sum_p\frac{L_p}{\omega^2-\omega_p^2}(\phi_1^p\phi_1^p-\phi_3^p\phi_3^p+\phi_6^p\phi_6^p-\phi_8^p\phi_8^p)\ ,$$

$$D=\sum_p\frac{L_p}{\omega^2-\omega_p^2}(\phi_1^p\phi_1^p+2\phi_2^p\phi_2^p+\phi_3^p\phi_3^p+\phi_6^p\phi_6^p+2\phi_7^p\phi_7^p+\phi_8^p\phi_8^p)\ ,$$

$$a_1=1-A,\quad a_2=1-D\ ,$$

$$a_3=1-\frac{\Omega^2}{\omega^2}-A,\quad a_4=1-\frac{\Omega^2}{\omega^2}-D\ ,$$

$$b_1^j=\sum_p\frac{\langle Q_p[[\sigma_2,\Lambda^p],\sigma_j]\rangle}{2\pi(\omega^2-\omega_p^2)}\ ,$$

$$b_2^j=\sum_p\frac{\omega_p\langle P_p[[\sigma_{10},\Lambda^p],\sigma_j]\rangle}{2\pi\omega(\omega^2-\omega_p^2)}\ ,$$

$$b_3^j=T_1^j+T_2^j+T_3^j\ ,$$

$$b_4^j=\frac{\omega}{i\Omega}T_1^j+\frac{\Omega}{i\omega}T_2^j+\frac{\omega}{i\Omega}T_3^j\ ,$$

$$T_1^j=\frac{\Omega}{\pi\omega^2}(n_0-n_1)\ ,$$

$$T_2^j=\sum_p\frac{\langle Q_p[[\sigma_7,\Lambda^p],\sigma_j]\rangle}{2\pi(\omega^2-\omega_p^2)}\ ,$$

$$T_3^j=\frac{i\Omega}{\omega}\sum_p\frac{\omega_p\langle P_p[[\sigma_{13},\Lambda^p],\sigma_j]\rangle}{2\pi\omega(\omega^2-\omega_p^2)}\ .$$

APPENDIX B

The definitions of terms used for the final evaluation of the spin Green functions [Eqs (5.11) and (5.12)] are as follows:

$$\alpha(\omega)=2n_1\omega^2D_t^2\sum_\lambda\delta^\lambda R_2^\lambda T_1^\lambda\ ,$$

$$\beta(\omega)=\pi n_1\omega^3D_t^2\sum_\lambda\delta^\lambda f_\lambda^2(\omega)T_1^\lambda\ ,$$

$$\Delta(\omega)=4\pi\omega^2D_t^2\sum_\lambda\delta^\lambda R_1^\lambda T_2^\lambda\ ,$$

$$\Gamma(\omega)=2\pi^2\omega^4D_t^2\coth\left[\frac{\hbar\omega}{2k_BT}\right]\sum_\lambda\delta^\lambda f_\lambda^2(\omega)T_2^\lambda\ ,$$

$$\alpha'(\omega)=\frac{\Omega}{\pi}(n_0-n_1)\ ,$$

$$\Delta'(\omega)=4\pi\omega^2D_t^2\sum_\lambda\delta^\lambda R_1^\lambda T_2^\lambda\ ,$$

$$\Gamma'(\omega)=2\pi^2\omega^4D_t^2\coth\left[\frac{\hbar\omega}{2k_BT}\right]\sum_\lambda\delta^\lambda f_\lambda^2(\omega)T_2^\lambda\ ,$$

$$\delta^\lambda=\frac{\hbar}{16\pi^3\rho_Mc_\lambda^5}\ ,$$

$$f_\lambda(\omega)=\left[1+\frac{a^{*2}}{4c_\lambda^2}\omega_\lambda^2\right]^{-2}\ ,$$

$$R_1^\lambda=\mathrm{P}\int_0^{\omega_D}\frac{x^3f_\lambda^2(x)\coth(\hbar x/2k_BT)}{\omega^2-x^2}dx\ ,$$

$$R_q^\lambda=\mathrm{P}\int_0^{\omega_D}\frac{x^2f_\lambda^2(x)}{\omega^2-x^2}dx\ ,$$

where P denotes principal value, ω_D denotes the Debye frequency, and

	$\lambda=l$	$\lambda=t_1$	$\lambda=t_2$
T_1^λ	$\frac{32}{45}$	$\frac{4}{9}$	$\frac{2}{3}$
T_2^λ	$\frac{16}{15}$	$\frac{4}{5}$	$\frac{8}{9}$

[1] B. L. Bird and N. Pearlman, Phys. Rev. B **4**, 4406 (1971).
[2] A. Adolf, D. Fortier, J. H. Albany, and K. Suzuki, Phys. Rev. Lett. **41**, 1477 (1978).
[3] A. Griffin and P. Carruthers, Phys. Rev. **131**, 1976 (1983).
[4] W. Kohn, Sol. State Phys. **5**, 258 (1957).
[5] R. W. Keyes, Phys. Rev. **122**, 1171 (1961).
[6] K. Suzuki and N. Mikoshiba, J. Phys. Soc. Jpn. **31**, 186 (1971).
[7] E. Sigmund, in *The Dynamical Jahn-Teller Effect in Localized Systems,* edited by Yu. Perlin and M. Wagner (North-Holland, Amsterdam, 1984).
[8] J. Maier and E. Sigmund, J. Phys. C **17**, 4141 (1984).
[9] J. Maier and E. Sigmund, *Proceedings of the Fourth International Conference on Phonon Scattering in Condensed Matter, Stuttgart, 1983,* edited by W. Eisenmenger, K. Lassmann, and S. Döttinger (Springer, Berlin, 1984).
[10] E. Sigmund and K. Lassmann, Phys. Status Solidi B **111**, 631 (1982).
[11] H. Fritzche, Phys. Rev. **125**, 1560 (1962).
[12] C. Hening and E. Vogt, Phys. Rev. **101**, 944 (1956).
[13] K. Suzuki, Phys. Status Solidi B **78**, K77 (1976).
[14] D. Schlechter, J. Phys. Chem. Solids **23**, 237 (1962).
[15] H. Hasegawa, Phys. Rev. **129**, 1029 (1963).
[16] J. Callaway, Phys. Rev. **113**, 1046 (1958).
[17] M. Klein, Phys. Rev. **186**, 839 (1969).
[18] M. Rueff, E. Sigmund, and M. Wagner, Phys. Status Solidi B **81**, 511 (1977).
[19] D. N. Zubarev, Fortschr. Phys. **9**, 275 (1961).
[20] K. Elk and W. Gasser, *Die Methode der Greenschen Funktionen in der Festkoerperphysik* (Akademie, Berlin, 1979).
[21] E. Sigmund and M. Wagner, Phys. Status Solidi B **57**, 635 (1973).
[22] E. Sigmund and M. Wagner, Z. Phys. **268**, 245 (1974).
[23] P. G. Klemens, Solid State Phys. **7**, 1 (1958).